JACS
JOURNAL OF THE AMERICAN CHEMICAL SOCIETY
Article
pubs.acs.org/JACS

Catalytic Production of Hydrogen Peroxide and Water by Oxygen-Tolerant [NiFe]-Hydrogenase during H_2 Cycling in the Presence of O_2

Lars Lauterbach[†,‡,§] and Oliver Lenz*[,†,§]

[†]Institut für Biologie/Mikrobiologie, Humboldt-Universität zu Berlin, Chausseestrasse 117, 10115 Berlin, Germany
[‡]Inorganic Chemistry Laboratory, Department of Chemistry, University of Oxford, South Parks Road, Oxford, OX1 3QR, United Kingdom
[§]Institut für Chemie, Sekretariat PC14, Technische Universität Berlin, Straße des 17. Juni 135, 10623 Berlin, Germany

Supporting Information

ABSTRACT: Hydrogenases control the H_2-related metabolism in many microbes. Most of these enzymes are prone to immediate inactivation by O_2. However, a few members of the subclass of [NiFe]-hydrogenases are able to convert H_2 into protons and electrons even in the presence of O_2, making them attractive for biotechnological application. Recent studies on O_2-tolerant membrane-bound hydrogenases indicate that the mechanism of O_2 tolerance relies on their capability to completely reduce O_2 with four electrons to harmless water. In order to verify this hypothesis, we probed the O_2 reduction capacity of the soluble, NAD^+-reducing [NiFe]-hydrogenase (SH) from *Ralstonia eutropha* H16. A newly established, homologous overexpression allowed the purification of up to 90 mg of homogeneous and highly active enzyme from 10 g of cell material. We showed that the SH produces trace amounts of superoxide in the course of H_2-driven NAD^+ reduction in the presence of O_2. However, the major products of the SH-mediated oxidase activity was in fact hydrogen peroxide and water as shown by the mass spectrometric detection of $H_2{}^{18}O$ formed from H_2 and isotopically labeled $^{18}O_2$. Water release was also observed when the enzyme was incubated with NADH and $^{18}O_2$, demonstrating the importance of reverse electron flow to the [NiFe] active site for O_2 reduction. A comparison of the turnover rates for H_2 and O_2 revealed that in the presence of twice the ambient level of O_2, up to 3% of the electrons generated through H_2 oxidation serve as "health insurance" and are reused for O_2 reduction.

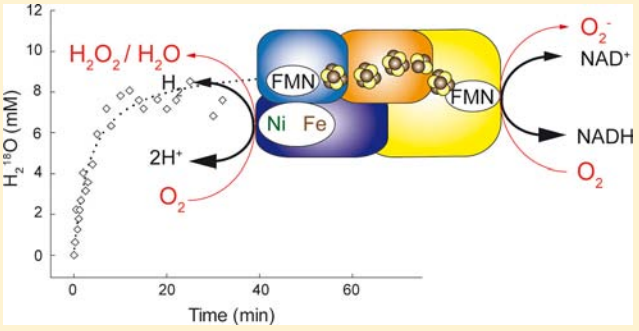

INTRODUCTION

The rapid and reversible interconversion between molecular hydrogen (H_2) and protons and electrons is widely used in nature and catalyzed by the enzyme hydrogenase. These biocatalysts are widespread in microbes, including bacteria, archaea, and lower eukarya, and depending on the metabolic context, are involved either in H_2 uptake for energy generation or in H_2 evolution to dissipate excess reducing power.[1] Hydrogenases are metalloenzymes occurring in different forms and are classified on the basis of the metal content in their catalytic center into [Fe]-, [FeFe]-, and [NiFe]-hydrogenases.[2] Because H_2 activation involves transition metals and low potential electrons, most hydrogenases are highly susceptible to oxidation by O_2, which inactivates the enzymes either reversibly or irreversibly.[3] Depending on the availability of electrons, different reactive oxygen species (ROS) can be generated at the active site upon O_2 reduction (Scheme 1).

Hydroxyl radicals represent clearly the most dangerous ROS, followed by superoxide and hydrogen peroxide. The four-electron reduction of O_2, however, yields harmless water. The likely reason for hydrogenase inactivation is the reaction of ROS with the catalytic center or other metal cofactors in the enzyme. This includes the production of deleterious hydroxyl radicals as a result of the Fenton reaction of H_2O_2 with ferric iron.

Scheme 1. Oxygen Species Produced upon Partial and Full Reduction of O_2

$$O_2 + e^- \rightarrow O_2^-$$

$$O_2 + 2\,e^- + 2\,H^+ \rightarrow H_2O_2$$

$$O_2 + 3\,e^- + 3\,H^+ \rightarrow H_2O + OH^-$$

$$O_2 + 4\,e^- + 4\,H^+ \rightarrow 2\,H_2O$$

Compared to the extremely O_2-sensitive [FeFe]-hydrogenases, the [NiFe]-hydrogenases are generally less affected by O_2. There are even some enzymes, called O_2-tolerant [NiFe]-hydrogenases, that catalyze hydrogen cycling in the presence of O_2. Prominent examples are the hydrogenases present in the soil bacterium *Ralstonia eutropha*,[4,5] Hyd-1 from *Escherichia coli*,[6] and hydrogen-converting catalysts from

Received: August 15, 2013
Published: November 1, 2013

   dx.doi.org/10.1021/ja408420d | *J. Am. Chem. Soc.* 2013, 135, 17897−17905

Aquifex aeolicus[7] and *Hydrogenovibrio marinus*.[8] Their capability to sustain H_2-cycling in the presence of O_2 has already been exploited in a number of biotechnological applications, such as enzymatic fuel cells, cofactor regeneration, and light-driven H_2 production.[9−11] In this respect, it is highly attractive to convert O_2-sensitive hydrogenases into O_2-tolerant enzymes.[12] Therefore, understanding the fundamentals of O_2 tolerance of certain hydrogenases is a matter of ongoing research.

Previous studies on the topic of O_2 tolerance were mainly dedicated to gas access to the active site via hydrophobic gas channels. Although restricted access of O_2 to the active site lowers the probability, it does not prevent the reaction with O_2 at the catalytic center.[13,14] The focus has changed only recently toward the idea of a catalytic detoxification of O_2 at the catalytic center. This idea is based on observations from chronoamperometric experiments done by the Armstrong group showing that O_2-tolerant, membrane-bound hydrogenases from *Ralstonia* species clearly react rapidly with O_2, but their H_2-oxidizing activity is nevertheless not completely inhibited.[15,16] This feature is consistent with the absence of the so-called Ni-A state, which is characterized by an oxygen-modified active site that is recalcitrant to rapid reactivation.[17] According to the current model, O_2 tolerance is mediated by the capability of the enzymes to deliver four electrons to the active site to completely reduce O_2 to harmless water.[18] In the case of O_2-tolerant membrane-bound [NiFe]-hydrogenases, this characteristic trait is crucially related to modifications of the primary electron-accepting/donating iron sulfur cluster close to the active site,[19] and indeed, crystal structures of the membrane-bound hydrogenases from *R. eutropha*, *H. marinus*, and *E. coli* uncovered an unprecedented [4Fe−3S] cluster at this position that shows striking redox-dependent structural changes.[20−22]

However, water production by O_2-tolerant [NiFe]-hydrogenases performing H_2 cycling in the presence of O_2 has not yet been proven. This is because the rate constant for the four-electron reduction of O_2 to water has been estimated to lie in the range of 10^{-1}−10^{-2} s^{-1}.[18] Hence, high amounts of enzyme and sensitive analysis methods are required for the reliable detection of water release. Moreover, most hydrogenases, which have been removed from their cellular context, require artificial electron donors/acceptors for in vitro catalysis. These are often redox dyes that themselves react with oxygen and, as a result, hamper O_2 reduction measurements.

Therefore, we focused our attention on the soluble, NAD^+-reducing [NiFe]-hydrogenase (SH) from the soil bacterium *Ralstonia eutropha* (Figure 1). This particular protein is seemingly the ideal candidate for the analysis of H_2-driven formation of ROS for three reasons. First, the protein sustains 100% of its H_2-driven NAD^+ reduction activity in the presence of atmospheric O_2 concentration.[23] Second, the substrates NAD^+ and NADH are stable in the presence of O_2. Third, the SH represents approximately 5% of the cytoplasmic protein and can be purified in large amounts.[24]

From a structural and functional perspective, the SH is closely related to the peripheral arm of Complex I.[25] However, in contrast to the NADH/ubiquinone oxidoreductase activity performed by the latter, the SH couples the oxidation of H_2 with the reduction of NAD^+. Under certain conditions, the enzyme is also capable of catalyzing the reverse reaction, the NADH mediated reduction of protons to H_2.[26] This is consistent with recent electrochemical experiments showing that the SH performs catalysis at minimal overpotential.[27,28]

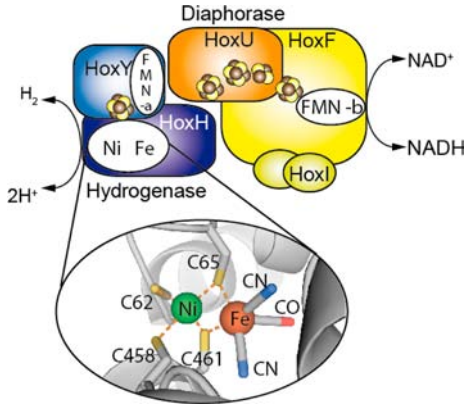

Figure 1. Modular structure and predicted cofactor composition of the soluble, NAD^+-reducing [NiFe]-hydrogenase of *R. eutropha*. For sake of clarity, the SH hydrogenase moiety (blue) and the diaphorase moiety (orange/yellow) are drawn separately. The SH contains one flavin mononucleotide (FMN) in each module. The electron-conducting iron−sulfur clusters are shown as cluster-forming brown/yellow spheres. A homology model (based on the crystal structure of the hydrogenase *Desulfovibrio vulgaris* Miyazaki F[29]) of the H_2-cycling [NiFe] active site in the hydrogenase module is shown in the blow-up. The coordination of the nickel and iron ions by four cysteinyl residues is indicated by dashed orange lines.

The different functions of the peripheral part of Complex I and SH are mainly based on the replacement of the quinone binding site in Complex I by a Ni−Fe center responsible for H_2 activation in the SH. Thus, the SH basically consists of two catalytic moieties, namely, a NADH/acceptor oxidoreductase (diaphorase) module, composed of the subunits HoxF and HoxU, and a heterodimeric hydrogenase module comprising subunits HoxH and HoxY (Figure 1). The [NiFe] catalytic center located in the HoxH subunit is linked to the NAD^+-binding site in the HoxF subunit by a series of [4Fe−4S] and [2Fe−2S] clusters and two flavin mononucleotide molecules, designated to as FMN-a (flavin mononucleotide a) and FMN-b (flavin mononucleotide b).[4] While FMN-b is a constituent of the NAD(H) binding site in the diaphorase module, FMN-a has been reported to be only loosely bound to the hydrogenase module.[27,28,30]

It has been shown previously that the [NiFe] site of SH is inactivated reversibly by O_2.[30] Incubation of the catalytically active SH hydrogenase module HoxHY with O_2 at high redox potential causes a slow enzyme inactivation, but activity is recovered within seconds when the redox potential is poised below −170 mV, even if O_2 is still present. This behavior is consistent with the rapid reactivation of the oxygen-inactivated active site by NADH which has been observed for the SH enzyme.[31,32] Interaction of O_2 with the [NiFe] center is also supported by infrared spectroscopic investigations on native SH residing in whole cells. The reversible formation of an active site species has been observed that was assigned to an oxidatively modified catalytic center.[33]

Like Complex I, the SH has been shown to release superoxide during catalysis in the presence of O_2.[23] In fact, superoxide production by Complex I is considered to be the major origin of cellular oxidative stress and causative for human diseases.[34,35] In this study we provide experimental evidence that the SH from *R. eutropha* also generates, besides superoxide, hydrogen peroxide and water as catalytic byproducts during H_2 and NADH conversion in the presence of O_2.

EXPERIMENTAL SECTION

Plasmid Construction, Growth Conditions, and Protein Purification. Strains and plasmids used in this study are listed in Table S1 in the Supporting Information. The expression plasmid employed for overproduction of the *Strep*-tagged SH from *R. eutropha* H16 was constructed as follows. Plasmid pGE770, containing the *hoxFUHYWIhypA*$_2$*B*$_2$*F*$_2$*CDEXhoxABCJ* genes under control of the native SH promoter served as the basis for the subsequent cloning steps. The *hoxF* gene was equipped at the 5′ end with a *Strep*-tag II-encoding sequence. The regulatory genes *hoxBC* and *J*, which are not required for SH gene expression, were eliminated by transferring a 15.3 kbp HindIII fragment from pGE770 to the HindIII-treated plasmid pCH1596. Plasmid pCH1596 had been constructed by inserting a 1.6 kbp SpeI-EcoRI fragment from pCH646 into SpeI-EcoRI-cut Litmus28. From the resulting plasmid pCH1595, a 20 kbp SpeI-XbaI fragment was transferred to pEDY309 cut with SpeI and XbaI. This step yielded plasmid pGE771, which was transferred via conjugation from *E. coli* S17-1 to the megaplasmid-free strain *R. eutropha* HF210.

For SH^{wt} purification, strain *R. eutropha* (pGE771) was grown heterotrophically in a mineral salts medium essentially as described in ref 36. The medium contained a mixture of 0.05% (w/v) fructose and 0.4% (v/v) glycerol and, in addition, 1 μM $NiCl_2$, 40 μM $FeCl_3$, 1 μM $ZnCl_2$, and the trace element solution SL6.[37] A culture volume of 4 L was shaken in baffled 5 L Erlenmeyer flasks at 120 rpm until the culture reached an optical density at 436 nm of 10 ± 1. Cells were harvested by centrifugation at 6000*g* for 12 min at 4 °C. For SH purification, the cells were resuspended in two volumes of 50 mM K-PO_4 buffer, pH 7.0, containing 5% glycerol and 5 mM NAD^+ and a protease inhibitor cocktail (EDTA-free protease inhibitor, Roche). The cell suspension was intensively flushed with argon. Cells were broken by two passages through a chilled French pressure cell at 6.2 MPa, and the resulting extract was centrifuged at 100 000*g* for 45 min. The suspension was maintained under an argon atmosphere. The resulting extract containing soluble proteins was applied to a *Strep*-Tactin Superflow column (IBA). The column was washed aerobically with 12 mL of resuspension buffer and subsequently with 18 mL of NAD^+-free resuspension buffer. Protein bound to the column was eluted with NAD^+-free resuspension buffer containing 5 mM desthiobiotin. Elution fractions containing SH protein were pooled and concentrated with an Amicon Ultra-15 device (100 kDa exclusion size, Merck Millipore, Germany). Cell cultivation and purification of the SH^{FU} variant were performed as previously described.[27]

Enzyme Assays. All enzyme measurements were performed in the presence of defined gas mixtures unless stated otherwise. Prior to use in enzyme assays, the buffers were bubbled with the respective gases. Buffers with 100% gas saturation (1 bar) contained 760 μM H_2, 1150 μM O_2, or 571 μM N_2. Buffers containing gas mixtures were prepared by mixing appropriate buffers with 100% gas saturation. The head space of the reaction vessels was filled with same gas mixture as present in the reaction buffer. The reactions were started with the addition of enzyme.

H_2-driven NAD^+ reduction of purified SH in soluble extracts was determined at 30 °C in a rubber-stoppered cuvette containing gassed 50 mM Tris-HCl buffer, pH 8.0, containing 1 μM FMN, 1 mM dithiothreitol (DTT), and 1 mM NAD^+.[31] Whole-cell activity measurements were done with cells treated with cetyltrimethylammonium bromide as described previously.[38]

NADH-driven H_2 production was measured in a sealed vial containing 100 μL of Tris-HCl buffer, pH 8.0, with 1 mM NADH, 1 μM FMN, 1 mM TCEP (tris(2-carboxyethyl)phosphine), and 55 μg of SH protein in the presence of either 100% N_2 or 40% O_2 and 60% N_2. Aliquots were withdrawn at different time points from the gas phase and analyzed by gas chromatography (Shimadzu GC-2014AT equipped for the detection of small gases with Hayesep N columns and a 13× molecular sieve column according to specification A0608005).

Diaphorase activity of the SH was measured anaerobically as NADH-dependent benzyl viologen reduction at 30 °C in 50 mM Tris-HCl buffer, pH 8.0, containing 5 mM benzyl viologen, 1 mM NADH, and 90 μM dithionite.[27]

SH-mediated oxygen reduction during H_2-driven NAD^+ reduction was quantified at 30 °C in a Clark electrode. The assay chamber was filled with 1.3−1.5 mL of Tris-HCl buffer (50 mM, pH 8.0) containing 40% O_2 and 60% H_2, 1 mM NAD^+, 1 μM FMN, and 1 mM TCEP. NADH-dependent oxygen reduction was assayed in buffer containing 40% O_2 and 60% N_2 and 1 mM NADH as the substrate.

Superoxide formation was measured by the O_2^--mediated oxidation of hydroxylamine to nitrite which was subsequently quantified according to a modified protocol of Schneider and co-workers.[23] Measurements were done at 30 °C in 5.2 mL sealed glass vials containing a reaction mixture of 450−1000 μL. The reaction mixture consisted of 50 mM Tris-HCl buffer, pH 8.0, 1 mM NAD^+, 1 μM FMN, 1 mM TCEP, 0.5 mM hydroxylamine hydrochloride, and 20−50 μg of SH protein. In the case of H_2-dependent measurements, the buffer contained 40% O_2, 60% H_2, and 1 mM NAD^+. NADH-dependent measurements were done in buffer containing 40% O_2, 60% N_2, and 1 mM NADH. At various time points, 33 μL samples were withdrawn and the reaction was stopped by the addition of 33 μL of α-naphthylamine (2.33 mM) and 33 μL of sulfanilic acid (6.33 mM). After 20 min, the nitrite concentration was determined by measuring the absorption at 530 nm. In the case of NADH-dependent superoxide production measurements, the reaction mixture contained buffer with 40% O_2, 60% N_2, and 1 mM NADH.

Hydrogen peroxide formation was quantified by the H_2O_2-mediated oxidation of 10-acetyl-3,7-dihydroxyphenoxazine (Sigma) to resofurin catalyzed by horseradish peroxidase (HRP). Measurements were done at 30 °C in 5.2 mL sealed glass vials containing a reaction mixture of 600 μL. The reaction mixture contained 50 mM Tris-HCl buffer, pH 8.0, 1 μM FMN, and 10−50 μg of SH protein. In the case of H_2-dependent measurements, the buffer contained 40% O_2 and 60% H_2 and 1 mM NAD^+. NADH-dependent measurements were done in buffer containing 40% O_2, 60% N_2, and 1 mM NADH. DTT and TCEP were omitted, as they interfere with the subsequent H_2O_2 determination. The 50 μL samples were withdrawn at different time points, and reaction was stopped by heating at 80 °C for 2 min. The sample was cooled to room temperature, and subsequently 50 μL of 50 mM Tris-HCl buffer, pH 8.0, containing 100 μM 10-acetyl-3,7-dihydroxyphenoxazine and 10 mU HRP was added. After incubation at room temperature for 30 min, the 10-acetyl-3,7-dihydroxyphenoxazine oxidation product resorufin was quantified by fluorescence measurements (excitation at 530 nm and emission at 590 nm). A calibration curve was taken by performing the assay with different H_2O_2 concentrations. Addition of HRP was essential to show that the SH cannot oxidize 10-acetyl-3,7-dihydroxyphenoxazine. As NADH and FMN interfere with 10-acetyl-3,7-dihydroxyphenoxazine, the background fluorescence of a reaction assay containing all ingredients except SH was used as a control.

$H_2{}^{18}O$ release as a result of SH-mediated reductive conversion of $^{18}O_2$ was quantified with a quadrupole mass spectrometer (Pfeiffer OmniStarTM GSD 301). Measurements were done at 30 °C in 5.2 mL sealed glass vials containing a reaction mixture of 30−100 μL. The reaction mixture contained 50 mM Tris-HCl buffer, pH 8.0, 1 μM FMN, 1 mM TCEP, and 50−90 μg of SH protein. In the case of H_2-dependent measurements, the buffer contained 1 mM NAD^+, 40% $^{18}O_2$ (99% Sigma), and 60% H_2. NADH-dependent measurements were done in buffer containing 100 mM NADH, 40% $^{18}O_2$, and 60% N_2.

At various time points, 10 μL samples were withdrawn and the water was subsequently evaporated at 100 °C for 20 min in a sealed 1.5 mL tube with an ice-cold lid. The water condensed at the bottom side of the lid was collected by centrifugation (4000*g*, 1 min) in a new reaction tube. This procedure prevented the blockage of the mass spectrometer capillary by salts, chemicals, or protein. An amount of 7 μL of the condensate was directly applied to the opening of the heated (160 °C) capillary. The flow rate was approximately 4 mL/min. Ions with a *m*/*z* of 2 (H_2), 18 ($H_2{}^{16}O$), 20 ($H_2{}^{18}O$), 32 ($^{16}O_2$), 36 ($^{18}O_2$), 38 ($H_2{}^{18}O_2$), 44 (CO_2) were recorded. TCEP-HCl as the main electron source for $^{18}O_2$ reduction can be excluded because the

dx.doi.org/10.1021/ja408420d | J. Am. Chem. Soc. 2013, 135, 17897−17905

maximum amount of detected $H_2{}^{18}O$ exceeded the amount of TCEP-HCl by a factor of 70 (not shown; in this case an amount of 1000 μg of SH protein was used). The linear phase of the production of reduction oxygen species was used for the calculation of the corresponding rates. The same time period was used for the determination of the O_2 reduction rate.

Protein and FMN Determination and Immunological Assays. The protein concentration was determined with the BCATM protein assay reagent kit (Pierce, USA) using bovine serum albumin as the standard. The flavin mononucleotide concentration in protein samples was analyzed fluorometrically as described previously.[30] SDS−PAGE was performed according to Laemmli et al.[39] For immunological detection of SH-related proteins, the following antisera were applied in the indicated dilutions: anti-HoxH antiserum (1:833), anti-HoxY antiserum (1:1666), anti-HoxF antiserum (1:2000), anti-HoxU antiserum (1:1666), anti-HoxI antiserum (1:5000).

RESULTS

Overexpression Constructs for the Assessment of the O_2-Reduction Capacity of the SH. The net O_2 reduction rate of the SH has been determined previously to be 2 orders of magnitude lower than the H_2-driven NAD^+ reduction activity.[32] For a reliable determination of the individual reduced oxygen species produced, we have designed a new homologous expression system allowing for SH overproduction in *R. eutropha*. The membrane-bound [NiFe]-hydrogenase (MBH) operon of *R. eutropha*, which comprises all genes required for synthesis of active hydrogenase even in heterologous hosts,[40] served as the blueprint for the construction. The megaplasmid-borne SH operon *hoxFUYHWIhypA*$_2$*B*$_2$*F*$_2$ of *R. eutropha* was cloned and subsequently amended by the *hypCDEXhoxA* gene cluster fragment of the MBH operon as described in Experimental Section. Furthermore, a sequence encoding the *Strep*-tag II peptide was attached to the 5′ end of the *hoxF* gene. The resulting synthetic *hox*$_{strep}$*FUYHWIhypA*$_2$*B*$_2$*F*$_2$*CDEXhoxA* operon was inserted into the broad-host range vector pEDY309 resulting in plasmid pGE760, encoding *Strep*-tagged wild-type SH (SH^{wt}). In order to narrow down the sites at which O_2 reduction takes place, the isolated *Strep*-tagged HoxFU diaphorase module of the SH, henceforth designated as SH^{FU}, was employed. This version, encoded on plasmid pGE533, harbors only the FMN-containing NAD^+ binding site and a series of FeS clusters but lacks the entire hydrogenase module.[27]

For enzyme purification, plasmid pGE760 was transferred into the hydrogenase-negative strain *R. eutropha* HF210, while pGE553 was established in *R. eutropha* HF424, as described previously.[27] The transconjugant strain *R. eutropha* HF210 (pGE760) was cultivated heterotrophically under oxygen-limited conditions,[19] which led to high SH activities of approximately 19 units per milligram of total protein measured as H_2-driven NAD^+ reduction in soluble cell extracts. The SH^{wt} protein was purified to homogeneity by *Strep*-Tactin affinity chromatography. From 10 g (wet weight) of cells, we routinely obtained 30−90 mg of protein with a specific H_2-driven NAD^+ reduction activity of 101 ± 32 units/mg of protein (Table S2 in the Supporting Information). The reverse reaction, namely, NADH-driven H_2 production, was catalyzed with an activity 0.078 ± 0.053 units/mg. These activities are comparable to those described in the literature.[23,24,31,32] SDS−PAGE in conjunction with immunological analyses performed with the SH^{wt} enzyme revealed five protein bands assigned to the SH subunits HoxFUHYI (Figure S1 in the Supporting Information). H_2-driven NAD^+ reduction activity of the wild-type enzyme increased by 100% through addition of flavin mononucleotide (FMN, Table S3 in the Supporting Information), which is consistent with previous findings suggesting the reconstitution of weakly bound FMN-a into the enzyme.[28] A 2-fold increase in activity was also observed upon addition of either dithiothreitol (DTT) or the O_2-insensitive reducing agent tris(2-carboxyethyl)phosphine hydrochloride TCEP-HCl (Table S3 in the Supporting Information). Furthermore, the time of linearity of the enzyme reaction was increased significantly in the presence of either the reducing agent or supplementary FMN. Because of their positive effects on SH activity, TCEP-HCl and FMN were added to all subsequent enzyme assays if not stated otherwise.

In order to test the functionality of the HoxFU diaphorase moiety in the SH derivatives, the NADH/benzyl viologen (BV) oxidoreductase activity was determined. The diaphorase activity for the SH^{wt} protein was 104.2 ± 6.2 units/mg of protein. The isolated SH^{FU} module, which was purified by affinity chromatography as described previously,[27] displayed a specific NADH/benzyl viologen oxidoreductase activity of 133.3 ± 25.6 units/mg of protein.

Net O_2 Reduction Activity of the SH. In the first instance, we determined the impact of O_2 on the H_2-driven NAD^+ reduction activity of the SH^{wt} enzyme. The addition of increasing amounts of O_2, i.e., 20%, 40%, 60%, and 80% (equivalent to 0.23, 0.46, 0.7, and 0.93 mM O_2, respectively, in solution), to the reaction mixture led to a prolongation of the lag phase of the reaction (Figure S2 in the Supporting Information), which corresponds to the time required for reactivation of the oxidized active site.[32] However, in the presence of 20% O_2, the H_2-driven NAD^+ reduction activity was almost the same as in the absence of O_2 (Table S4 in the Supporting Information). Even at the highest O_2 concentration of 80%, the activity decreased by only about 20% compared to anaerobic assay conditions, which is in accordance with previous observations[23] and underlines the extraordinary O_2 tolerance of the SH. In order to obtain sufficient amount of potential products resulting from O_2 reduction, all subsequent measurements were performed at a concentration of 40% O_2. The net O_2 reduction activity of the SH variants was quantified with a Clark electrode (Figure 2A). In the presence of 40% O_2, the SH^{wt} protein displayed an H_2-mediated O_2 reduction activity of 0.52 ± 0.09 units/mg when NAD^+ was added to the reaction. In the absence of the substrate NAD^+ (despite the presence of 1 mM TCEP and 5 μM FMN), no O_2 reduction activity was detectable showing that H_2-driven NAD^+ reduction is required for the oxidase activity of the enzyme. O_2 was also reduced through reverse electron flow, i.e., upon incubation of the SH variants with 1 mM NADH. However, for unknown reasons, the O_2 reduction activity during NADH oxidation was not sufficiently linear within the time period of 15 min of the measurement (Figure 2B). Therefore, we have determined the apparent O_2 reduction rates considering the first 5−10 min of the reaction. This allowed a suitable comparison with the production rates of the products from O_2 reduction, which are described below. The apparent NADH-driven O_2 reduction rates determined for the SH^{wt} and SH^{FU} proteins were 94 ± 17 and 31 ± 2 min^{-1}, respectively (Table 1). Notably, in the presence of 40% O_2, the H_2 production rate of the SH^{wt} enzyme amounted to 6.7 ± 1.2 min^{-1}.

Superoxide Production during Catalysis. The results described above clearly show that both H_2 and NADH serve as potent electron donors for O_2 reduction. Further experiments

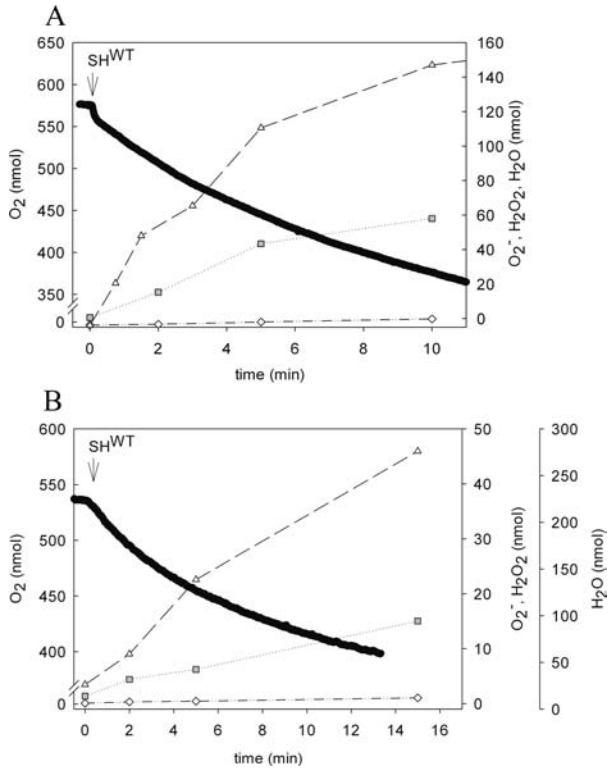

Figure 2. Rates of superoxide, hydrogen peroxide, and water formation in comparison to the O_2 reduction rate. The measurements were done in the presence of FMN for both H_2-driven NAD^+/O_2 reduction (A) and NADH-driven proton/O_2 reduction (B) as described in Experimental Section. The data were normalized to the SH protein amount used for O_2 reduction measurements (39 μg). Rates were determined using the data time periods between 0 and 5 min or between 0 and 10 min, depending on linearity. Note that the reaction started only upon addition of the enzyme: open diamonds, superoxide; gray squares, hydrogen peroxide, open triangles, water; dark circles (continuous measurement), dioxygen.

were undertaken to identify the individual reduced oxygen species produced by the enzyme. We first focused our attention on superoxide, which has been previously shown to be responsible for SH inactivation.[23] Superoxide formation was monitored by an established assay that exploits the superoxide-dependent oxidation of hydroxylamine to nitrite.[41] By using H_2 as the electron donor in combination with NAD^+ and O_2 as electron acceptors, we observed a relatively low superoxide production rate of 1.1 min^{-1} for the SH^{wt} protein (Table 1), which is in the same range as the published value of 0.5 min^{-1}.[32] Reverse electron flow, i.e., NADH-mediated O_2 reduction resulted in superoxide production rates of 0.45 and 0.46 min^{-1} for the SH^{wt} and SH^{FU} proteins, respectively.

Hydrogen Peroxide Production during Catalysis. The superoxide production activity of the SH^{wt} enzyme was 2 orders of magnitude lower than the O_2 reduction activity. This implies that ROS other than superoxide represent the main products released upon O_2 reduction. Therefore, we analyzed the capacity of the SH to produce hydrogen peroxide, which is generated by a two-electron reduction of dioxygen (Scheme 1). H_2O_2 production was quantified by the horseradish peroxidase-mediated oxidation of 10-acetyl-3,7-dihydroxyphenoxazine. The hydrogen peroxide production activity of the SH^{wt} protein in the presence of H_2 and NAD^+ was 0.27 units/mg. This value corresponds to a turnover rate of 55 min^{-1}, which is ~100-fold higher than the corresponding superoxide production rate (Figure 2A, Table 1). In this respect it is important to mention that superoxide disproportionates spontaneously into hydrogen peroxide and oxygen.[42] H_2O_2 production rates were also measured for both SH variants using NADH as the electron donor (Figure 2B, Table 1). A rate of ~6 min^{-1} was determined for the SH^{wt} protein, showing that hydrogen peroxide is also produced by reverse electron flow. Interestingly, the SH^{FU} variant displayed only a very low H_2O_2 production rate of 0.2 min^{-1} which is by a factor of 30 lower than that of wild-type SH. This revealed that the hydrogenase module is the major player in SH-mediated H_2O_2 production.

Water Production during Catalysis. Among the products of O_2 reduction, water is clearly the least reactive one. In order to test whether water is a product of the O_2 reduction capability of the SH, we have established an experimental setup that allows reliable detection and quantification of isotopically labeled $H_2{}^{18}O$ as a catalysis product from hydrogenase. An amount of 50−1000 μg of SH was mixed with 1 mM NAD^+ in a small buffer volume of 30−100 μL, which was placed in a gastight, rubber-sealed reaction vessel filled with 40% (v/v) $^{18}O_2$ and 60% (v/v) H_2. In the case of using NADH as the electron donor, the same amount of enzyme was incubated with 100 mM NADH under a gas atmosphere of 40% (v/v) $^{18}O_2$ and 60% (v/v) N_2. At various time points, an amount of 10 μL of the reaction mixtures was withdrawn and gas analysis was performed with a mass spectrometer as described in the Experimental Section. This method allowed the reliable detection of concentration changes of 1.8 mM $H_2{}^{18}O$ (Figure

Table 1. Net O_2 Turnover Rate and the Individual Production Rates for Superoxide, Hydrogen Peroxide, and Water for the SH Variants under Different Reaction Conditions

protein		net O_2 reduction (min^{-1})[a]	O_2^- production (min^{-1})	H_2O_2 production (min^{-1})[b]	$H_2{}^{18}O$ production (min^{-1})
Reaction Direction: $H_2 \rightarrow NAD^+/{}^{(18)}O_2$					
SH^{wt}	+FMN	109 ± 19	1.1 ± 0.1	55 ± 7	122 ± 8
	−FMN	76.3 ± 7.8	0.6 ± 0.2	17.9 ± 5.8	74.6 ± 19.5
Reaction Direction: NADH $\rightarrow {}^{(18)}O_2$[c]					
SH^{wt}	+FMN	94 ± 17	0.45 ± 0.11	5.8 ± 0.6	116 ± 9
	−FMN	49 ± 10	nd	14.2 ± 0.2	31.4 ± 7.0
SH^{FU}	+FMN	31 ± 2	0.46 ± 0.04	0.2 ± 0.1	67 ± 10
	−FMN	20.7 ± 2	nd	0.1 ± 0.1	32.1 ± 1

[a]Reduction/production rates were measured in the presence of 40% O_2 as described in the Experimental Section. Values represent the arithmetic mean and the respective standard deviation of three independent experiments. [b]The addition of catalase (100 units) to the reaction prevented the formation of resorufin, underlining the specificity of the assay for H_2O_2. [c]No $H_2{}^{18}O$ production was detectable in the absence of NADH.

dx.doi.org/10.1021/ja408420d | J. Am. Chem. Soc. 2013, 135, 17897−17905

S3 in the Supporting Information) within the natural abundance of 111 mM $H_2{}^{18}O$.[43]

Upon incubation with H_2, NAD^+, and $^{18}O_2$, the SH^{wt} protein displayed a considerable $H_2{}^{18}O$ production activity of 0.60 ± 0.04 units per milligram of protein. This value corresponds to a turnover rate of 122 min^{-1} (Table 1), which remained linear for 5−7 min (Figure 2A). The net amount of the detected water also included H_2O that was produced indirectly from the thermal decomposition of superoxide and H_2O_2. However, the NADH-dependent $H_2{}^{18}O$ production rate of the wild-type SH was 20- and 258-fold higher than the H_2O_2 and superoxide production rates, respectively. This implies that $H_2{}^{18}O$ is the major byproduct released by the SH in the course of H_2-driven NAD^+ reduction and the thermal decomposition of ROS does not play a significant role in water production. The latter was confirmed by analyzing and comparing the superoxide, hydrogen peroxide, and water production rates of the well-established ROS-producing enzyme xanthine oxidase. The H_2O_2 production rate was 3-fold higher than the water production rate, which indicates that the thermal decomposition of H_2O_2 is minimal (Table S5 in the Supporting Information).

In subsequent experiments, we investigated the $H_2{}^{18}O$ production capacity of the SH variants incubated with NADH in the presence of $^{18}O_2$. Using NADH as the electron donor resulted in a turnover rate of 116 min^{-1} for the SH^{wt} protein (Table 1). This rate is very similar to that obtained for the SH^{wt} enzyme during H_2 oxidation in the presence of NAD^+ and $^{18}O_2$. In order to get a hint as to whether $H_2{}^{18}O$ release takes place in the diaphorase module, the hydrogenase module, or both, the SH^{FU} variant was tested for its $H_2{}^{18}O$ production capacity. In fact, the SH^{wt} and SH^{FU} proteins displayed similar $H_2{}^{18}O$ production activities of 567 and 686 nmol·min^{-1}·mg^{-1}. However, considering the difference in size (205 kDa for SH^{wt} and 110 kDa for SH^{FU}), the SH^{FU} variant had an approximately 2-fold lower $H_2{}^{18}O$ production rate of 67 min^{-1} compared to the wild-type protein (116 min^{-1}). These results suggest that NADH-driven $H_2{}^{18}O$ production takes place in both SH modules of the SH.

If all products of O_2 reduction are captured quantitatively by the different assays, all oxygen atoms of the reduced O_2 molecules should appear as constituents of the products. In the case of the H_2-driven NAD^+ reduction catalyzed by the SH^{wt} protein, approximately 50% of the O_2-derived oxygen atoms were found in H_2O_2 while the other half was deposited in form of water. During NADH oxidation in the presence of O_2, the SH^{wt} protein released 62% of the oxygen atoms in the form of water and only 6% as H_2O_2. In all test cases, arithmetically 60−110% of the O_2-derived O atoms were recovered in the form of H_2O and H_2O_2; only 1% was found to be incorporated in superoxide molecules. The deviation from 100% is most likely caused by inaccuracies of the intricate H_2O measurement, for which the relatively high abundance of $H_2{}^{18}O$ in normal water must be taken into account.

Role of FMN in H_2O_2 and H_2O Production. The experiments shown above suggest that O_2 reduction leads to water formation in both SH modules, while superoxide is produced mainly in the diaphorase module and hydrogen peroxide primarily released within the hydrogenase module. It is well-known that reduced flavins are capable of the formation of ROS including H_2O_2.[34] Purified SH^{wt} enzyme contained only 1.00 ± 0.08 instead of the two proposed FMN molecules. However, the obvious loss of flavin is in line with previous observations and has been explained by the release FMN-a from the hydrogenases module in the course of the purification process.[28,30,44] van der Linden and co-workers showed that the cofactor can be reconstituted in the enzyme simply by the addition of free FMN to the purified protein.[44]

In order to test the role of FMN-a in the hydrogenase moiety of the SH, we determined the production of reduced oxygen species in the absence of externally added FMN both for the H_2 oxidation and NADH oxidation directions. By omission of FMN in the assays, the O_2 reduction rate dropped by 30−50% for both SH variants (Table 1). This indicated that even the FMN-b in the SH^{FU} protein is not bound stably, which corroborated recent results.[27] In the case of NADH oxidation, the decrease in O_2 reduction activity was accompanied by a 50% drop of H_2O release by the SH^{FU} module. Under the same conditions, the lack of external FMN resulted in a residual activity of only 27% for the SH^{wt} protein. This further supports the conclusion that H_2O production takes place in both the hydrogenase and diaphorase module of the SH. Interestingly, the NADH-driven H_2O_2 production activity of SH^{wt} protein increased from 5.8 ± 0.6 milliunits in the presence of 1 μM FMN to 14.2 ± 0.2 milliunits per milligram of protein in the absence of external FMN. The decrease of H_2O_2 production in the presence of FMN was accompanied by an increase in $H_2{}^{18}O$ production (Table 1). These observations suggest that in the case of NADH oxidation, the presence of FMN-a in the hydrogenase module shifts the H_2O/H_2O_2 production ratio toward water. However, this effect of FMN was not observed when the SH^{wt} protein catalyzed H_2-driven NAD^+ reduction. The superoxide, hydrogen peroxidase, and water production rates decreased concomitantly with the O_2 reduction activity in the case when FMN was not added externally.

■ DISCUSSION

In order to assess quantitatively the products of the O_2 reduction activity of the soluble, NAD^+-reducing [NiFe]-hydrogenase (SH) from *R. eutropha*, we have designed a new plasmid-based overexpression system. This system is based on a generic operon comprising all genes necessary for synthesis of catalytically active SH. The attachment of a *Strep*-tag II peptide to the N-terminus of the HoxF subunit allowed a rapid and mild purification of highly active SH, and the protein yield was 10-fold higher than previously reported.[24] The H_2-driven NAD^+ reduction activity was 101 units/mg, which corresponds to a turnover rate of 342 s^{-1} for the heterohexameric SH^{wt} protein with an apparent molecular weight of 205 kDa. In the presence of 0.47 mM O_2 (40% saturation), the rate decreased by only 15% to a final rate of 289 s^{-1}, demonstrating the extraordinary O_2 tolerance of the enzyme. Under the same conditions, a net O_2 reduction rate of 1.8 s^{-1} was determined showing that the SH^{wt} reacts continuously with both H_2 and O_2. Thus, the conversion of approximately 150 H_2 molecules is accompanied by the reduction of one molecule of O_2, assuming a complete reduction to H_2O.

It is important to note that when fueled by NADH, the O_2 reduction rate (1.6 s^{-1}) of the SH^{WT} protein in the presence of 40% O_2 was 15-fold higher than the corresponding H_2 production rate (0.11 s^{-1}). This is consistent with a model in which H^+ and O_2 compete for the electrons at the [NiFe] active site, and because of thermodynamic reasons, O_2 is clearly preferred. It has been shown previously that the SH serves as an H_2-evolving electron valve in vivo when *R. eutropha* cells are shifted from aerobic to anaerobic conditions.[26] The SH possibly

dx.doi.org/10.1021/ja408420d | J. Am. Chem. Soc. 2013, 135, 17897−17905

also contributes to the NADH-driven removal of O_2 during this transition phase, thereby regenerating NAD^+. A comparable function has been described for the water-producing NADH oxidase II from *Streptococcus mutans*.[45]

In the course of analysis of the products of O_2 reduction by the SH, we were able to detect superoxide, hydrogen peroxide, and water. The most reactive species, superoxide, was produced only in trace amounts in relation to the net O_2 reduction rate. Both the SH^{wt} and SH^{FU} proteins produced superoxide at similar rates of approximately 0.5 min^{-1}. This supports the previous finding that the diaphorase module of the SH accommodates the site of superoxide production.[27] Consistent with observations for Complex I, it is likely that single electron transfer from reduced FMN to O_2 in the NAD^+/NADH binding pocket results in the formation of superoxide. SH-mediated superoxide production in vivo is reflected by the up-regulation of the detoxifying enzyme superoxide dismutase during lithoautotrophic growth of *R. eutropha* on H_2 and CO_2 in the presence of O_2.[46]

The two-electron reduction of O_2 results in the formation of H_2O_2, which was detected at a rate of 55 min^{-1} during H_2-driven NAD^+ reduction by the SH^{wt} enzyme. Ten times less but still significant amounts of H_2O_2 production were observed with the SH^{wt} working in the reverse direction, i.e., during NADH oxidation in the absence of H_2. Under the same conditions, however, the SH^{FU} module released H_2O_2 only in trace amounts. This clearly shows that hydrogen peroxide is mainly produced in the hydrogenase module. SH-mediated release of hydrogen peroxide is consistent with the up-regulation of the H_2O_2-detoxifying proteins iron-dependent peroxidase and catalase which has been observed in *R. eutropha* cells grown on H_2, CO_2, and O_2.[46] In this context, it should be noted that the oxidized SH has been shown to be relatively stable in the presence of 10 mM H_2O_2 under nonturnover conditions.[23]

So far, a conventional iron−sulfur cluster has not been identified as the source of H_2O_2, whereas FMN is a well-known cofactor that can be involved in H_2O_2 production.[47] According to previous observations, FMN-a is only loosely bound to the SH^{wt} protein. FMN-a-depleted protein fails to catalyze H_2-driven NAD^+ reduction. However, it can easily be reconstituted by the addition of external FMN.[28,44] We observed that the O_2 reduction rate of the SH^{wt} enzyme as well as the superoxide, H_2O_2, and H_2O production rates decreased by 30−70% in the absence of externally added FMN, which is entirely consistent with the previous findings. By contrast, during NADH oxidation, the FMN-depleted SH^{wt} protein showed a 2-fold higher H_2O_2 production rate than its FMN-loaded counterpart. This suggests that hydrogen peroxide is not produced directly at the FMN-a cofactor, leaving the catalytic center as a possible site of H_2O_2 release. The production of H_2O, however, which requires two further electrons, was positively dependent on the presence of FMN. These observations are in line with the assumption that the supplemented flavin refills the partially empty FMN-a-binding sites in the enzyme and serves as electron mediator. In this context, free FMN is not involved in H_2O_2 release, since neither O_2 reduction nor ROS production was observed in protein-free but FMN-containing reaction assays.

The presence of FMN as a two-electron carrier close to the soluble hydrogenase active site is analogous to the situation in O_2-tolerant membrane-bound [NiFe]-hydrogenases. Crystal structures of these enzymes revealed the presence of a novel [4Fe−3S] cluster species close to the catalytic center.[20−22] It is assumed that this cofactor can undergo two rapid, consecutive one-electron transfer reactions that assist in the reductive removal of oxygen species at the active site.[19] The current model of oxygen tolerance for membrane bound [NiFe]-hydrogenases suggests complete reduction of O_2 to water with four electrons and four protons. On the basis of an O_2 attack on the active site with a vacant binding site (Ni_a−S state), the electron demand can be accomplished by one electron from Ni^{II}, two electrons from the fully reduced [4Fe−3S] cluster, and one electron from the remaining Fe−S cluster chain.[18,19]

In the case of the O_2-tolerant SH, the situation seems to be different in two aspects. First, the function of the [4Fe−3S] cluster in membrane-bound enzymes might be taken over by FMN-a. Second, in contrast to MBH proteins, the SH resides in the cytoplasm, which provides a reducing environment. Consistently, in situ spectroscopic studies on the SH located in intact cells revealed the reduced Ni_a−C state of the active site as resting state, even in the absence of H_2.[33] The constant supply of low levels of NADH results in the presence of two electrons in the form of a bridging hydride at the active site. These two electrons are readily available in the case of O_2 attack and would be sufficient, in combination with one proton, to convert O_2 into a hydroperoxo ligand. Upon protonation the ligand can be released as H_2O_2. Such a scenario is documented in Figure 3. Interestingly, the insertion of molecular oxygen in transition metal hydride bonds and the concomitant formation of metal hydroperoxide have been shown for several, especially nickel hydride-containing, model complexes.[48] The presence of a peroxo species bound to the active site of as-isolated, oxidized SH has already been proposed by Albracht and co-workers[49] and would explain the need for reductive reactivation of

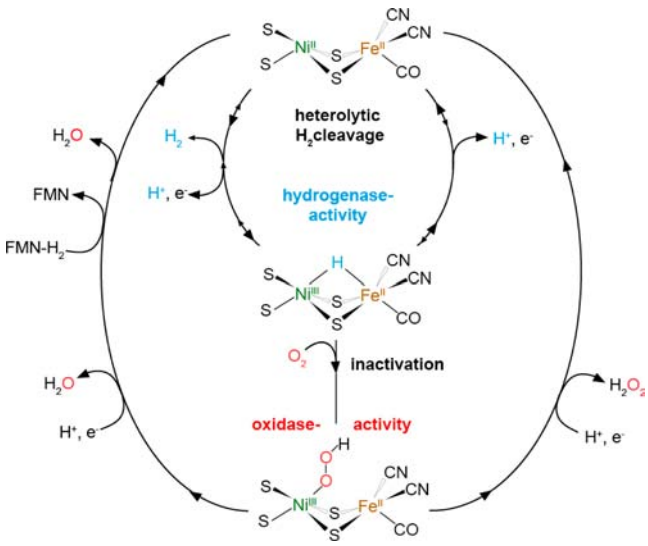

Figure 3. Model of H_2 oxidation and O_2 reduction at the SH active site. The active site structure of the SH in the N_{ia}−S state is shown at the top. Incubation with either H_2 or NADH reveals the Ni_a−C state that is characterized by a bridging hydride between Ni and Fe. In the presence of O_2 the bridging hydride donates two electrons, resulting in a proposed hydroperoxo ligand. Upon protonation the ligand is released as H_2O_2 (right circle). Three protons and two further electrons, which may be derived from reduced FMN-a, lead to the formation of two H_2O molecules (left circle). For both reactions a further electron is required to reenter the Ni_a−S state. The Ni_a−C state is regenerated by the subsequent incubation with H_2 or NADH.

dx.doi.org/10.1021/ja408420d | J. Am. Chem. Soc. 2013, 135, 17897−17905

the enzyme by NADH through reverse electron flow. Three protons and two further electrons, the latter may derive from FMN-a, are required to fully reduce the two oxygen atoms of the proposed hydroperoxo species into two harmless water molecules (Figure 3).

Our data show that water and H_2O_2 represent the major products of O_2 reduction by the native SH enzyme. However, it is important to note that the isolated SH^{FU} module showed a considerable H_2O production from $^{18}O_2$ and NADH. Similar to the flavoprotein subcomplex of Complex I,[50] the SH^{FU} unit contains flavin and Fe−S clusters. In the case of *Bos taurus* Complex I, it has been shown that the reduced flavin is capable of transferring electrons to oxygen to primarily form superoxide.[42] In contrast, Complex I from *E. coli* releases mainly hydrogen peroxide.[34] To our knowledge water production as a result of O_2 reduction has not been tested so far for any isolated Complex I fragment. In the case of SH^{FU}, reduced FMN-b and two further electrons from reduced Fe−S clusters would be sufficient to reduce oxygen completely to water. However, metal cofactors are not necessarily required for NADH-dependent production of H_2O from O_2. In the case of the H_2O-forming NAD(P)H oxidase from *Lactobacillus sanfranciscensis*, one NAD(P)H molecule binds to the active site and transfers the hydride to an enzyme-bound FAD.[51] O_2 is then being reduced to H_2O_2 which is immediately decomposed to a water molecule, while the remaining oxygen atom is bound to a conserved cysteine residue, thereby forming a Cys−S−OH intermediate. With the aid of a second NAD(P)H the sulfenic acid is back-converted to a thiolate and a second H_2O molecule is released. The NADH peroxidase from *Enterococcus faecalis* seems to employ a comparable mechanism.[52] It is conceivable that a similar mechanism is responsible for H_2O production in vicinity to the FMN-b cofactor of SH^{FU}. However, according to the amino acid composition of the SH^{FU} active site region, there is no potential redox-active cysteine residue that can fulfill the acceptor role for H_2O_2. Another possibility would be water production at a metal cluster that is exposed to the protein surface of HoxFU as a result of the detachment from the HoxHY module. Because of their spatial arrangement, the most likely candidates would be the two [4Fe−4S] clusters in HoxU that are homologous to the clusters N_4 and N_5 in Complex I.[25,53] It is important to mention that there is so far no known iron−sulfur cluster that catalyzes directly the reduction of O_2 to H_2O. Thus, site and mechanism of H_2O release by SH^{FU} remain elusive and require further investigation.

CONCLUSIONS

Our data suggest that O_2 reduction occurs at multiple sites in the SH, albeit it is impossible, at the current stage, to define these sites on an atomic level. However, with regard to the necessity of preventing active site damage, it is rather likely that H_2O and H_2O_2 release, as a result of O_2 reduction, takes place in the vicinity of or directly at the catalytic [NiFe] center of native SH. A small fraction of the electrons produced during H_2 cleavage is being reused in order to reduce O_2. Two concurrent electron transfer steps (supported by a metal-bound hydride and a fully reduced FMN cofactor) prevent the formation of the most reactive O_2^- and OH^- species at the [NiFe]-active site. In fact H_2O_2 and harmless water are the major products of O_2 detoxification. Thus, the SH possesses both hydrogenase and oxidase activities. These findings are notably important for engineering O_2-tolerant hydrogenases and for the design of chemical, transition metal-based catalysts, which are usually highly sensitive to oxygen.

ASSOCIATED CONTENT

Supporting Information

Tables S1−S5 and Figures S1−S3. This material is available free of charge via the Internet at http://pubs.acs.org.

AUTHOR INFORMATION

Corresponding Author

oliver.lenz@tu-berlin.de

Notes

The authors declare no competing financial interest.

ACKNOWLEDGMENTS

L. Lauterbach was supported by ERC Proof of Concept Grant 297503. The work was supported by the ERC Proof of Concept Grant 297503 (to L.L.) and the Deutsche Forschungsgemeinschaft (DFG) through the Cluster of Excellence "Unifying Concepts in Catalysis", Berlin (to L.L. and O.L.). We are indebted to Tanja Burgdorf for construction of plasmid pGE770 and to Stefan Frielingsdorf for excellent technical support in MS analysis. We thank Kylie Vincent, Marius Hoch, Leland B. Gee, Ingo Zebger, and Bärbel Friedrich for helpful discussions and generous support.

REFERENCES

(1) Schwartz, E.; Fritsch, J.; Friedrich, B. In *The Prokaryotes: Prokaryotic Physiology and Biochemistry*, 4th ed.; DeLong, E. F., Lory, S., Stackebrandt, E., Thompson, F., Rosenberg, E., Eds.; Springer-Verlag: Berlin, 2013; p 119.

(2) Vignais, P. M.; Billoud, B. *Chem. Rev.* **2007**, *107*, 4206.

(3) Fontecilla-Camps, J. C.; Volbeda, A.; Cavazza, C.; Nicolet, Y. *Chem. Rev.* **2007**, *107*, 4273.

(4) Horch, M.; Lauterbach, L.; Lenz, O.; Hildebrandt, P.; Zebger, I. *FEBS Lett.* **2012**, *586*, 545.

(5) Lenz, O.; Ludwig, M.; Schubert, T.; Burstel, I.; Ganskow, S.; Goris, T.; Schwarze, A.; Friedrich, B. *ChemPhysChem* **2010**, *11*, 1107.

(6) Lukey, M. J.; Parkin, A.; Roessler, M. M.; Murphy, B. J.; Harmer, J.; Palmer, T.; Sargent, F.; Armstrong, F. A. *J. Am. Chem. Soc.* **2010**, *285*, 3928.

(7) Pandelia, M. E.; Fourmond, V.; Tron-Infossi, P.; Lojou, E.; Bertrand, P.; Leger, C.; Giudici-Orticoni, M. T.; Lubitz, W. *J. Am. Chem. Soc.* **2010**, *132*, 6991.

(8) Nishihara, H.; Miyashita, Y.; Aoyama, K.; Kodama, T.; Igarashi, Y.; Takamura, Y. *Biochem. Biophys. Res. Commun.* **1997**, *232*, 766.

(9) Vincent, K. A.; Cracknell, J. A.; Clark, J. R.; Ludwig, M.; Lenz, O.; Friedrich, B.; Armstrong, F. A. *Chem. Commun. (Cambridge, U. K.)* **2006**, *48*, 5033.

(10) Ratzka, J.; Lauterbach, L.; Lenz, O.; Ansorge-Schumacher, M. B. *Biocatal. Biotransform.* **2011**, *29*, 246.

(11) Krassen, H.; Schwarze, A.; Friedrich, B.; Ataka, K.; Lenz, O.; Heberle, J. *ACS Nano* **2009**, *3*, 4055.

(12) Liebgott, P. P.; de Lacey, A. L.; Burlat, B.; Cournac, L.; Richaud, P.; Brugna, M.; Fernandez, V. M.; Guigliarelli, B.; Rousset, M.; Leger, C.; Dementin, S. *J. Am. Chem. Soc.* **2011**, *133*, 986.

(13) Liebgott, P. P.; Leroux, F.; Burlat, B.; Dementin, S.; Baffert, C.; Lautier, T.; Fourmond, V.; Ceccaldi, P.; Cavazza, C.; Meynial-Salles, I.; Soucaille, P.; Fontecilla-Camps, J. C.; Guigliarelli, B.; Bertrand, P.; Rousset, M.; Leger, C. *Nat. Chem. Biol.* **2010**, *6*, 63.

(14) Leroux, F.; Dementin, S.; Burlat, B.; Cournac, L.; Volbeda, A.; Champ, S.; Martin, L.; Guigliarelli, B.; Bertrand, P.; Fontecilla-Camps, J.; Rousset, M.; Leger, C. *Proc. Natl. Acad. Sci. U.S.A.* **2008**, *105*, 11188.

(15) Vincent, K. A.; Cracknell, J. A.; Lenz, O.; Zebger, I.; Friedrich, B.; Armstrong, F. A. *Proc. Natl. Acad. Sci. U.S.A.* **2005**, *102*, 16951.

(16) Vincent, K. A.; Parkin, A.; Lenz, O.; Albracht, S. P.; Fontecilla-Camps, J. C.; Cammack, R.; Friedrich, B.; Armstrong, F. A. *J. Am. Chem. Soc.* **2005**, *127*, 18179.
(17) Saggu, M.; Teutloff, C.; Ludwig, M.; Brecht, M.; Pandelia, M. E.; Lenz, O.; Friedrich, B.; Lubitz, W.; Hildebrandt, P.; Lendzian, F.; Bittl, R. *Phys. Chem. Chem. Phys.* **2010**, *12*, 2139.
(18) Cracknell, J. A.; Wait, A. F.; Lenz, O.; Friedrich, B.; Armstrong, F. A. *Proc. Natl. Acad. Sci. U.S.A.* **2009**, *106*, 20681.
(19) Goris, T.; Wait, A. F.; Saggu, M.; Fritsch, J.; Heidary, N.; Stein, M.; Zebger, I.; Lendzian, F.; Armstrong, F. A.; Friedrich, B.; Lenz, O. *Nat. Chem. Biol.* **2011**, *7*, 310.
(20) Fritsch, J.; Scheerer, P.; Frielingsdorf, S.; Kroschinsky, S.; Friedrich, B.; Lenz, O.; Spahn, C. M. *Nature* **2011**, *479*, 249.
(21) Shomura, Y.; Yoon, K. S.; Nishihara, H.; Higuchi, Y. *Nature* **2011**, *479*, 253.
(22) Volbeda, A.; Amara, P.; Darnault, C.; Mouesca, J. M.; Parkin, A.; Roessler, M. M.; Armstrong, F. A.; Fontecilla-Camps, J. C. *Proc. Natl. Acad. Sci. U.S.A.* **2012**, *109*, 5305.
(23) Schneider, K.; Schlegel, H. G. *Biochem. J.* **1981**, *193*, 99.
(24) van der Linden, E.; Burgdorf, T.; de Lacey, A. L.; Buhrke, T.; Scholte, M.; Fernandez, V. M.; Friedrich, B.; Albracht, S. P. *J. Biol. Inorg. Chem.* **2006**, *11*, 247.
(25) Albracht, S. P. J.; Hedderich, R. *FEBS Lett.* **2000**, *485*, 1.
(26) Kuhn, M.; Steinbüchel, A.; Schlegel, H. G. *J. Bacteriol.* **1984**, *159*, 633.
(27) Lauterbach, L.; Idris, Z.; Vincent, K. A.; Lenz, O. *PLoS One* **2011**, *6*, e25939.
(28) Schneider, K.; Schlegel, H. G. *Biochem. Biophys. Res. Commun.* **1978**, *84*, 564.
(29) Ogata, H.; Mizoguchi, Y.; Mizuno, N.; Miki, K.; Adachi, S.; Yasuoka, N.; Yagi, T.; Yamauchi, O.; Hirota, S.; Higuchi, Y. *J. Am. Chem. Soc.* **2002**, *124*, 11628.
(30) Lauterbach, L.; Liu, J. A.; Horch, M.; Hummel, P.; Schwarze, A.; Haumann, M.; Vincent, K. A.; Lenz, O.; Zebger, I. *Eur. J. Inorg. Chem.* **2011**, *2011*, 1067.
(31) Burgdorf, T.; van der Linden, E.; Bernhard, M.; Yin, Q. Y.; Back, J. W.; Hartog, A. F.; Muijsers, A. O.; de Koster, C. G.; Albracht, S. P. J.; Friedrich, B. *J. Bacteriol.* **2005**, *187*, 3122.
(32) Schneider, K.; Schlegel, H. G. *Biochim. Biophys. Acta* **1976**, *452*, 66.
(33) Horch, M.; Lauterbach, L.; Saggu, M.; Hildebrandt, P.; Lendzian, F.; Bittl, R.; Lenz, O.; Zebger, I. *Angew. Chem.* **2010**, *49*, 8026.
(34) Esterhazy, D.; King, M. S.; Yakovlev, G.; Hirst, J. *Biochemistry* **2008**, *47*, 3964.
(35) Hirst, J. *Biochem. J.* **2010**, *425*, 327.
(36) Schwartz, E.; Gerischer, U.; Friedrich, B. *J. Bacteriol.* **1998**, *180*, 3197.
(37) Pfennig, N. *Arch. Microbiol.* **1974**, *100*, 197.
(38) Friedrich, B.; Heine, E.; Finck, A.; Friedrich, C. G. *J. Bacteriol.* **1981**, *145*, 1144.
(39) Laemmli, U. K. *Nature* **1970**, *227*, 680.
(40) Lenz, O.; Gleiche, A.; Strack, A.; Friedrich, B. *J. Bacteriol.* **2005**, *187*, 6590.
(41) Elstner, E. F.; Heupel, A. *Anal. Biochem.* **1976**, *70*, 616.
(42) Kussmaul, L.; Hirst, J. *Proc. Natl. Acad. Sci. U.S.A.* **2006**, *103*, 7607.
(43) Gonfiantini, R. *Nature* **1978**, *271*, 534.
(44) van der Linden, E.; Faber, B. W.; Bleijlevens, B.; Burgdorf, T.; Bernhard, M.; Friedrich, B.; Albracht, S. P. *Eur. J. Biochem.* **2004**, *271*, 801.
(45) Higuchi, M.; Yamamoto, Y.; Poole, L. B.; Shimada, M.; Sato, Y.; Takahashi, N.; Kamio, Y. *J. Bacteriol.* **1999**, *181*, 5940.
(46) Kohlmann, Y.; Pohlmann, A.; Otto, A.; Becher, D.; Cramm, R.; Lütte, S.; Schwartz, E.; Hecker, M.; Friedrich, B. J. *Proteome Res.* **2011**, *10*, 2767.
(47) Massey, V. J. *Biol. Chem.* **1994**, *269*, 22459.
(48) Schlangen, M.; Schwarz, H. *Helv. Chim. Acta* **2008**, *91*, 379.
(49) Burgdorf, T.; Löscher, S.; Liebisch, P.; Van der Linden, E.; Galander, M.; Lendzian, F.; Meyer-Klaucke, W.; Albracht, S. P. J.; Friedrich, B.; Dau, H.; Haumann, M. *J. Am. Chem. Soc.* **2005**, *127*, 576.
(50) Barker, C. D.; Reda, T.; Hirst, J. *Biochemistry* **2007**, *46*, 3454.
Happe, R. P.; Roseboom, W.; Egert, G.; Friedrich, C. G.; Massanz, C.; Friedrich, B.; Albracht, S. P. J. *FEBS Lett.* **2000**, *466*, 259.
(51) Lountos, G. T.; Jiang, R.; Wellborn, W. B.; Thaler, T. L.; Bommarius, A. S.; Orville, A. M. *Biochemistry* **2006**, *45*, 9648.
(52) Poole, L. B.; Claiborne, A. *J. Biol. Chem.* **1989**, *264*, 12330.
(53) Sazanov, L. A.; Hinchliffe, P. *Science* **2006**, *311*, 1430.